6th International Conference on Multiphase Flow,
ICMF 2007, Leipzig, Germany, July 9–13, 2007

Experimental study of bubble formation at porous spargers

Nikolaos A. Kazakis, Aikaterini A. Mouza and Spiros V. Paras

Aristotle University of Thessaloniki, Department of Chemical Engineering
Laboratory of Chemical Process and Plant Design
Univ. Box 455, GR 54124, Thessaloniki, Greece
paras@cheng.auth.gr

Keywords: bubble column, porous sparger, coalescence, visualization

Abstract

This work is a study of the effect of liquid properties and the operating conditions on the interactions between under-formation bubbles. Experiments were conducted in a cell equipped with two adjacent micro-tubes (i.d. 110 μm) for the gas injection whose relative position was 210, 700 and 1370 μm. This set-up simulates, though in a simplified manner, the porous sparger operation, and it is used to study the coalescence and breakage phenomena observed on its surface. Various liquids covering a wide range of surface tension and viscosity values are employed, while the gas phase is atmospheric air. A fast video recording technique is used for both the visual observations of the phenomena occurring onto the sparger and the bubble size measurements. The experiments show that the interactions between under-formation bubbles depend strongly on the liquid properties, the distance between the tubes and the gas flow rate.

Introduction

Bubble columns are widely used as gas-liquid contactors in many applications such as absorption, blood oxygenation, fermentations, bio-reactions, coal liquefaction and waste water treatment. Due to their simple construction, low operating cost, high energy efficiency and good mass and heat transfer, bubble columns offer many advantages when used as gas–liquid contactors. In all these processes gas holdup and bubble size are important design parameters, since they define the interfacial area available for mass transfer, while it is widely known that both are affected by the coalescence and breakage phenomena occurring inside the column.

Bubble interactions in bubble columns play a significant role in the column operation because they directly affect the bubble size. Many investigators (e.g. Marrucci & Nicodemo, 1967; Camarasa et al., 1999; Collela et al. 1999; Mouza et al., 2005) have studied how bubble size varies with the column height due to the aforementioned bubble interaction mechanisms. They studied the effect of the liquid properties, the gas flow rate and the type of gas sparger on bubble size distribution and they pointed out the importance of the phenomena occurring at the vicinity of the sparger in the determination of the bubble distribution along the column. Amongst the gas spargers used for the gas injection, the porous plates hold advantages over the other types of gas distributors, since they produce numerous and smaller bubbles and thus offering a greater gas/liquid contact area. However, information concerning this kind of sparger is limited.

In a recent study Kazakis et al. (2007) measured the initial bubble size distribution at relatively low gas flow rates in a bubble column equipped with a porous sparger and found that bubble development is controlled by the pore size distribution, the gas flow rate and the properties of the liquid phase and it depends extensively on phenomena occurring directly onto or in the vicinity of the sparger surface. In addition, meticulous visual observations of the bubble formation process on the porous sparger indicate that many neighboring pores contribute to a single bubble creation. Consequently, experiments focused on the phenomena occurring onto the sparger surface are essential in order to establish rigorous criteria for the coalescence and breakage of fluid objects at the microscopic level (Delhaye & McLaughlin, 2003).

Many investigators have tried to elucidate the coalescence and breakage phenomena by studying the effect of the flow field, the bubble size and the liquid properties on them. Most of the early studies were focused on the role of the bubble wake in coalescence of vertically aligned bubbles in various liquids (Crabtree & Bridgwater, 1971; Nevers & Wu, 1971; Dekee et al., 1986). These investigators suggest that the trailing bubble enters the wake of the leading bubble and accelerates towards it till collision occurs. This is followed by the thinning of the liquid film between them until complete coalescence, whose rate increases with the viscosity of the liquid phase.

In recent studies the interest was focused on the coalescence between two adjacent bubbles in a controlled envi-

ronment. For example, Tse et al. (1998) observed the stages of the coalescence process between two bubbles in a coalescence cell for water and a range of electrolyte solutions. The bubbles were formed at two horizontal nozzles facing each other and the observations were made by means of a high-speed camera. They concluded that the coalescence probability depends on the hydrodynamics of drainage and surface properties as well as on the external flow. The more vigorously bubbles are driven by that flow, the more rapidly the film drains and the more likely they are to coalesce, especially if they are hindered from bouncing apart. A few years later, the same group (Tse et al., 2003) observed that the coalescence of two bubbles can also result in the formation of a daughter one. This coalescence-linked breakage mechanism is more pronounced when the bubbles are large due to their increased flexibility as they are more susceptible to distortion. A similar experimental set-up was used by Zahradnik et al. (1999), who studied the effect of aliphatic alcohols in viscous saccharose solutions on bubble coalescence. They concluded that coalescence could be suppressed by the addition of small amounts of alcohols. However, it must be noted that the above investigators used nozzles with relatively large internal diameter (2 mm), while the use of *horizontal* nozzles does not adequately simulate an industrial sparger operation, since bubbles are forced to coalesce.

On the other hand, studies with interaction between bubbles growing on adjacent vertical nozzles have also been conducted. Marrucci (1969) proposed a theory of coalescence for two bubbles growing at neighboring nozzles and touching each other sideways. He claims that coalescence occurs in two stages: first the liquid film between the bubbles thins down to a quasi-equilibrium thickness and then ruptures after a specific time. Kim & Lee (1987) studied the effect of organic solutes on coalescence time between two bubbles growing on adjacent nozzles of internal diameter 1.65 mm and 0.85 mm apart. They found that the time required to achieve coalescence increases with increase of solute concentration. However, the quality of their pictures was rather poor. Duineveld (1998) studied the encounter of bubble pairs in water and aqueous surfactant solutions. The equally-sized bubbles were formed by two needles with various internal diameters (from 0.51 to 1.70 mm), but his observations were made in the area above the needles, *after* bubble detachment. He found that in pure water bubbles coalesce when the Weber number, based on the approach velocity, was below a critical value and bounce if this critical Weber number is exceeded. When surfactants added to water exceed a critical concentration, bubbles are prevented to coalesce. Recently, Tsang et al. (2004) studied the effect of the electrolyte concentration and bubble diameter on the interaction of a pair of bubbles with equal size grown on adjacent capillaries of 2.39 mm i.d. in aqueous magnesium sulfate solutions. They found that the time required for coalescence between the bubbles increases with the salt concentration and that smaller bubbles coalesce easier.

It must be noted that all the above studies have been conducted in a controlled environment, meaning that the two nozzles were independently supplied with the gas phase, resulting in the formation of two synchronous and equal-sized bubbles. However, this is not the case when a porous sparger is employed for the gas dispersion. Kazakis et al. (2007) have proved that the size of bubbles formed from a porous sparger depends on the pore size distribution and generally follows a unimodal or bimodal distribution. Prince & Blanch (1990) also accentuate that either the measurement of coalescence times in stagnant liquids or the determination of coalescence rates from bubble size data obtained in turbulent systems are not satisfactory approaches for determining the rate of coalescence under practical hydrodynamic conditions. Consequently, in order to study these phenomena in a microscope scale, conditions closer to "*reality*" are required.

This work is motivated by the findings of the previous works conducted in this laboratory (Mouza et al., 2005; Kazakis et al., 2007). Careful observations on the bubble formation have shown that the interactions between the under-formation bubbles depend on the distance between neighboring active pores. For example, it was observed that two closely adjacent pores may contribute to the formation of a single bubble, while two bubbles from more distant individual active sites may also interact during their expansion. The scope of the current work is to gain an insight into the mechanisms of coalescence and breakage phenomena, which take place onto the surface of a porous sparger between neighboring pores and they determine the size distribution in bubble columns. This is accomplished by conducting experiments in a microscopic scale. It is regarded that two neighboring pores can be adequately simulated by two adjacent tubes located at various distances between them so as the effect of the relative position of the pores on the bubble formation to be studied. A high speed camera is used to observe the interactions between bubbles produced by the two adjacent vertical micro-tubes for the various liquid phases, gas flow rates and distances between the tubes employed.

Nomenclature

a	major bubble axis (m)
b	minor bubble axis (m)
d_b	bubble diameter (m)
d_i	tube inside diameter (m)
L	tube length (m)
r	pore radious (m)
t	time (sec)

Greek letters

ΔP	capillary pressure (Pa)
μ	viscosity (Pa s)
ρ	density (kg/m^3)
σ	surface tension (N/m)

Subscripts

L	liquid phase

Experimental Facility

The experimental set-up is illustrated in **Fig. 1** and it consists of a small vertical rectangular Plexiglas® column (***cell***) with a square cross section of side length 4 cm and height 12 cm. To increase the total height of the column a cylindrical Plexiglas® pipe (6.5 cm i.d. and 35 cm height) was also adjusted at the top of the column. Two stainless steel micro-tubes of 110 μm i.d. (Hamilton®) and 6 cm long are

used for the gas injection installed at the centre of the bottom plate. This set-up is considered equivalent, though in a simplified manner, to a miniature segment of a porous sparger of the same material (**Fig. 2**).

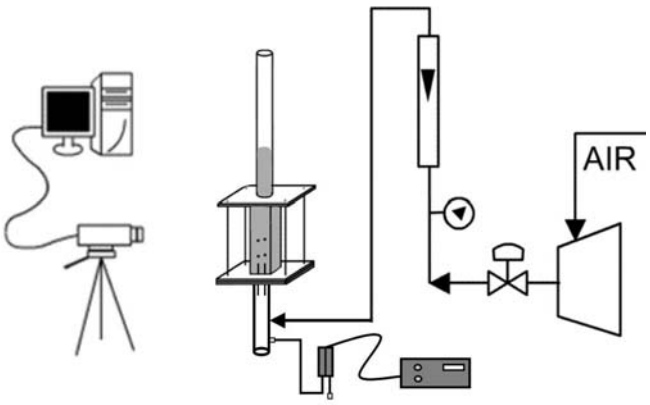

Figure 1: Experimental setup.

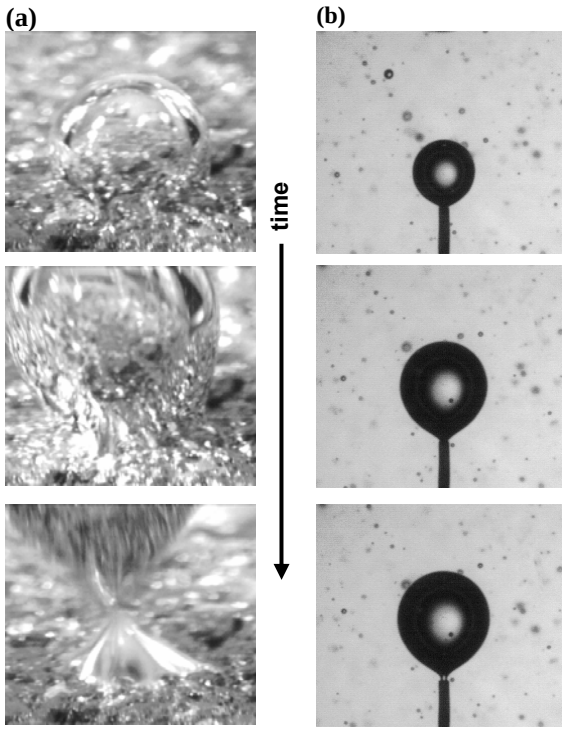

Figure 2. Instances of bubble formation at: (a) an active site of a porous sparger (Kazakis et al., 2007), (b) a 110 μm i.d. micro-tube.

Bubble growth on the tubes takes place under constant flow rate, since the ratio L/d_i^4 for each tube is 4.1×10^{14} m^{-3}, which satisfies the criterion proposed by Takahashi & Miyahara (1976). When a long thin capillary is employed for bubble injection, there is generally sufficiently high flow resistance in the tube such that the pressure gradient in the tube prevents events in the gas chamber upstream of the tube from interacting with the events at the bubble forming point (Kulkarni & Joshi, 2005). In this case, the size of the chamber has a negligible effect on the bubble formation mechanism. In addition, a common, for both tubes, gas chamber below the tubes is used, whose volume (120 ml) is very large compared to the diameter of the tubes, ensuring that no pressure variations occur during bubble formation (Kulkarni & Joshi, 2005). Consequently, constant flow conditions are achieved for the bubble formation whereas constant pressure conditions are obtained in the chamber (Khurana & Kumar, 1969).

The pressure inside the chamber is monitored by a differential pressure transducer (*Validyne® DP103*). The use of a common gas chamber is considered more appropriate for the simulation of a porous sparger, since, although pressure is common below the sparger surface, pores do not operate synchronously and with the same flow rate. Consequently, as gas flow rate inside each tube is not known a priori, it is calculated by measuring the volume of the bubbles produced at each tube for a certain time period. The total gas flow rate and, thus, the flow rate inside each tube, are controlled by varying the pressure inside the chamber.

All experiments were conducted at ambient pressure and temperature conditions (25±1 °C). The gas phase was air for all runs, while several liquids, i.e., water and various aqueous glycerin and isobutanol solutions, covering a sufficiently wide range of viscosity (1-16.6 mPa s) and surface tension values (49-72 mN/m) (**Table 1**), were employed as liquid phase. The height of the liquid phase during the experiments was 12 cm above the tubes. In order to simulate the operation of two equally sized pores at different locations on a porous sparger, three distances (i.e., 210, 700 and 1370 μm) between the tubes were tested. The gauge pressure inside the chamber was varied between 50–255 mbar corresponding to a total gas flow rate $1.6 \cdot 10^{-8}$ – $56 \cdot 10^{-8}$ m^3/s.

Table 1. Liquid phase properties at 25 °C.

Liquid phase	*Index*	μ_L (*mPa s*)	ρ_L (*kg/m^3*)	σ_L (*mN/m*)
water	*w*	1.0	997	72
aqueous iso-butanol solution 2.2% (v/v)	*i*	0.9	990	49
aqueous glycerin solution 33.3% (v/v)	*g1*	3.6	1080	70
aqueous glycerin solution 50.0% (v/v)	*g2*	6.2	1140	69
aqueous glycerin solution 66.7% (v/v)	*g3*	16.6	1180	67

A high-speed digital video camera (*Redlake MotionScope PCI® 1000S*) is employed in order to gain an insight into the coalescence/breakage phenomena occurring during bubble formation on the two tubes. The camera is fixed on a stand very close to the area of observation in such a way that the test section is located between the camera and an

appropriate lighting system placed behind a diffuser to evenly distribute the light. A recording rate of 500 fps is used during the experiments, while the shutter speed employed was of 1/5000. Using appropriate software (*Redlake MotionScope®*) the size of the bubbles and the coalescence time, defined as the time elapsed between the first contact of the bubbles and coalescence, can be obtained from the recorded images for the various liquids and flow conditions examined.

The known external diameter of the two tubes is used for the calibration of the measuring system and the accurate measurement of the bubble size. The bubbles are approximated by ellipsoids and the equivalent diameter of a sphere with the same volume as the ellipsoid is computed by the equation:

$$d_b = \sqrt[3]{a^2 b} \tag{1}$$

where d_b is the equivalent bubble diameter and a and b are the major and minor axes of the ellipsoid, respectively. The spatial resolution of the measuring technique is approximately 60 μm, while the maximum uncertainty in measuring the length of each axis of the bubbles, due to unavoidable shadows at the bubble interface, mainly at high gas flow rates, is of the order of 250 μm. Considering all the above, it is estimated that the the uncertainty of the measurements is less than 10%.

Results and Discussion

Effect of tube distance on bubble coalescence

It is generally accepted that coalescence occurs in three steps: i.e., collision, liquid film drainage and rupture of the film. When two bubbles collide, the liquid film formed by the small amount of liquid trapped between them begins to drain until it becomes sufficiently thin to be ruptured due to an instability mechanism. The above described sequence leads to a coalesced bubble.

Visual observations of the recorded images indicate that the distance between the tubes plays an important role on the coalescence probability between the forming bubbles, since it determines the:

- size at which bubbles come in contact,
- duration of this contact, before bubbles attain their final size and detach from the tubes and
- size of the resultant bubble, in case of coalescence.

The experiments in the microscopic scale revealed that there are three different types of coalescence between two bubbles growing at adjacent tubes. **Fig. 3** illustrates the bubble coalescence process for various liquids and distances between the tubes. Similar bubble interactions have also been observed by Kazakis et al. (2007) between bubbles forming on a porous sparger and they are also illustrated in **Fig. 3** for comparison.

The type of coalescence depends on the stage of bubble expansion at which bubbles coalesce. For the closest tube distance (**Fig. 3a**) bubbles come in touch and coalesce while being at the early stages of bubble expansion. It is widely known that, when coalescence occurs, the newly coalesced bubble is subjected to strong deformations. Since bubbles, in the case of the closest distance between the tubes, have relatively small size when coalescence occurs, the resultant bubble is also small and rigid and thus there are almost no oscillations due to bubble deformations (Tse et al., 2003). This allows the resultant bubble to remain attached to both tubes and to keep growing, while gas is being supplied by both tubes, until it reaches the final size and detachment occurs. A similar behaviour has also been observed between bubbles growing at very close sites, where after coalescence, the new bubble remains attached at both sites and keeps growing. However, when the distance between the two tubes is larger, bubbles have adequately increased their size before coalescence (**Fig. 3b**). Consequently, as soon as coalescence takes place, the new bubble is subjected to intense deformations, which do not allow it to remain attached to either tube. So, the size of the resultant bubble does not change further and it starts to ascend due to buoyancy. This type of coalescence has also been observed on the porous sparger surface (**Fig. 3b**). Finally, coalescence between adjacently growing bubbles can also take place, while they are at the final instances of the expansion stage and prior to their detachment (**Fig. 3c**). This case is similar to the previous one, but the size of the newly coalesced bubble is larger and the deformations, just after the rupture of the liquid film between the two bubbles, are much stronger and continue while the bubble ascends. In the same figure (**Fig. 3c**), such event on the porous sparger surface is also observed. Two bubbles just prior to detachment, come in touch and coalesce giving a relatively large bubble which detaches from the sparger and oscillates while moving upward.

Apart from the aforementioned coalescence types, a coalescence dependent breakage mechanism has also been observed during the experiments. **Fig. 4** illustrates this mechanism for the various distances between the micro-tubes when water is used as the liquid phase. In this figure, one can see that at the moment of coalescence, a very small daughter bubble is also generated and ascends very slowly, affected by the surrounding flow field.

This mechanism has also been observed by Tse et al. (2003) and was explained as follows: coalescence-linked breakage occurs when the newly coalesced bubble is subjected to a considerable amount of distortion. The increased flexibility of larger bubbles, especially in air–water systems, may increase the susceptibility of the newly coalesced bubble to pronounced distortion. Following the coalescence process an annular wave is formed due to the very rapid expansion of the hole formed after the film rupture. As this wave moves along the length of the bubble, away from the point of rupture, it causes a rippling effect which distorts the newly formed bubble and may result in the formation of an unstable extension. Instabilities due to the annular wave pinch off a portion of this extension, resulting in the generation of a small daughter bubble (Tse et al., 2003).

A first observation is that the size of the daughter bubble seems to depend on the size of the coalescing bubbles. **Table 2** gives the size of the two bubbles just before coalescence and the size of the resulting daughter bubble, which is of the same order of magnitude with that observed by Tse et al. (2003). It is obvious that the size of the generated bubble increases as the size of the two bubbles increase. This is probably due to the increased deformation of the resultant bubble as its size augments. Another observation is that this daughter bubble is always generated from the side of the smaller bubble.

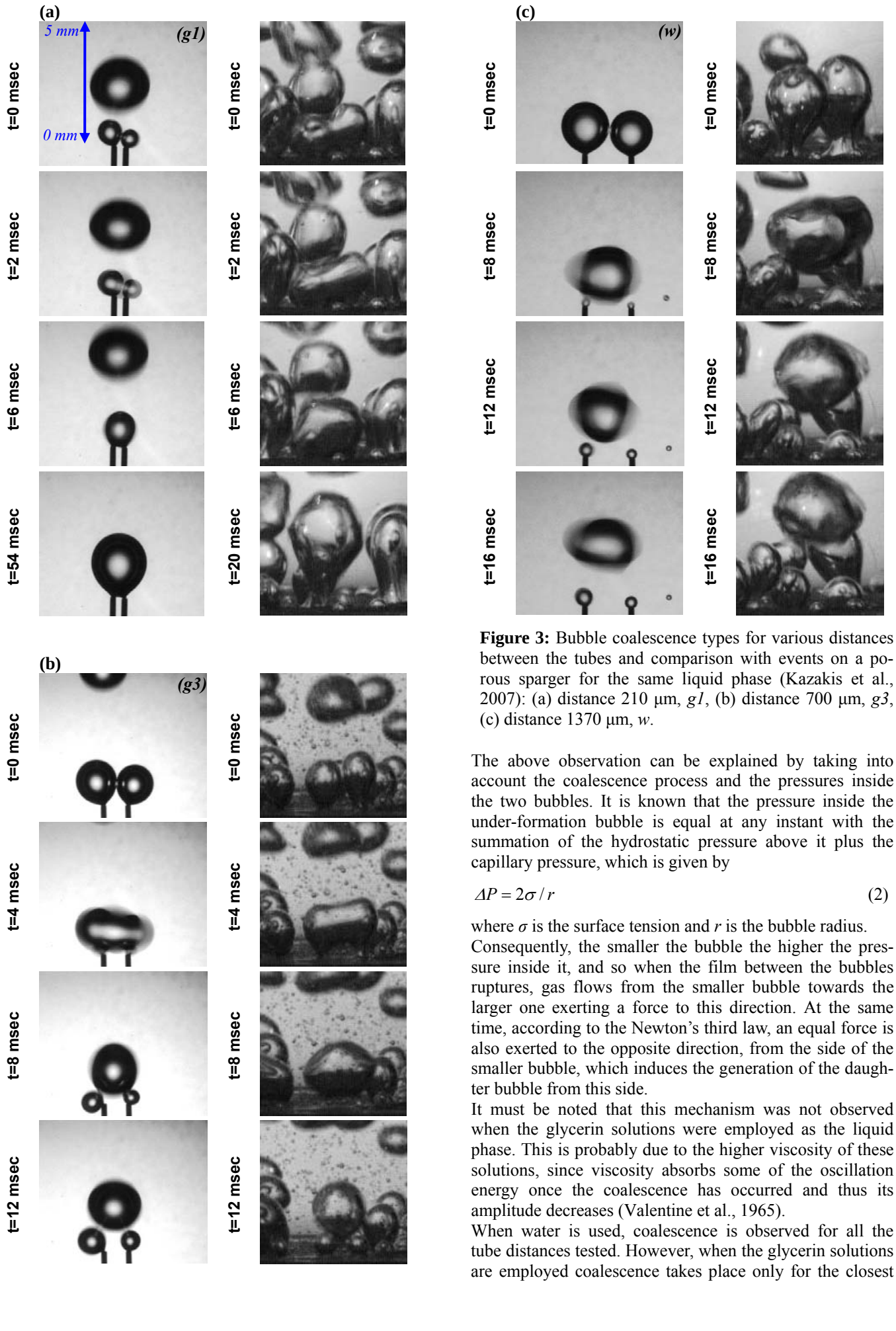

Figure 3: Bubble coalescence types for various distances between the tubes and comparison with events on a porous sparger for the same liquid phase (Kazakis et al., 2007): (a) distance 210 μm, *g1*, (b) distance 700 μm, *g3*, (c) distance 1370 μm, *w*.

The above observation can be explained by taking into account the coalescence process and the pressures inside the two bubbles. It is known that the pressure inside the under-formation bubble is equal at any instant with the summation of the hydrostatic pressure above it plus the capillary pressure, which is given by

$$\Delta P = 2\sigma / r \qquad (2)$$

where σ is the surface tension and r is the bubble radius. Consequently, the smaller the bubble the higher the pressure inside it, and so when the film between the bubbles ruptures, gas flows from the smaller bubble towards the larger one exerting a force to this direction. At the same time, according to the Newton's third law, an equal force is also exerted to the opposite direction, from the side of the smaller bubble, which induces the generation of the daughter bubble from this side.

It must be noted that this mechanism was not observed when the glycerin solutions were employed as the liquid phase. This is probably due to the higher viscosity of these solutions, since viscosity absorbs some of the oscillation energy once the coalescence has occurred and thus its amplitude decreases (Valentine et al., 1965).

When water is used, coalescence is observed for all the tube distances tested. However, when the glycerin solutions are employed coalescence takes place only for the closest

distance (210 μm), while for the other distances almost no coalescence is observed, since the contact time between the bubbles is very small, as it will be discussed in the next section.

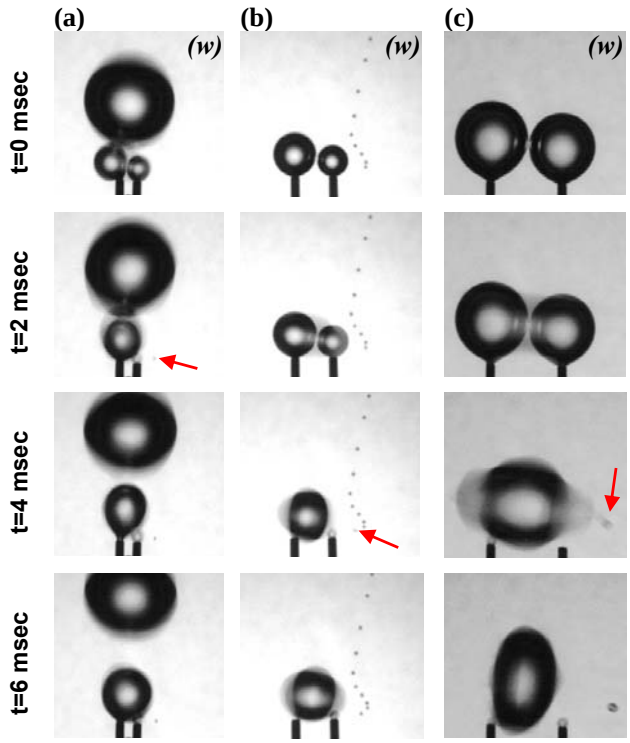

Figure 4: Coalescence-linked breakage mechanism for *w* and tube distance: (a) 210 μm, (b) 700 μm, (c) 1370 μm.

Table 2. Size of coalescing and daughter bubbles for various distances between the tubes.

Tube distance, (*μm*)	Size of large bubble, (*μm*)	Size of small bubble, (*μm*)	Size of daughter bubble, (*μm*)
210	700	500	~50
700	1000	800	~100
1370	1800	1600	~200

Effect of surface tension

In a previous work, Kazakis et al. (2007) have studied the effect of surface tension on the initial bubble size distribution on a porous sparger, i.e., the size distribution of the bubbles just after detachment (**Fig. 5**). It is obvious that, as the surface tension decreases the distribution curve is shifted to lower sizes. This is attributed to both the inhibition of coalescence of adjacently forming bubbles and the activation of more pores, since the capillary pressure (**Eq. 2**), which is the resistance to bubble formation, becomes smaller as surface tension decreases (Kazakis et al., 2007). This is also confirmed by the findings of the present study. An aqueous isobutanol solution was used in order to study the effect of surface tension on the interaction between the growing bubbles. The visual observations reveal that coalescence between the adjacent bubbles is always inhibited for the whole range of the gas flow rates employed, regardless of the contact time. As a result two bubbles of different size were always formed from the two tubes, which ascend after they reach their final size (**Fig. 6a**). In the same figure (**Fig. 6b**), the formation of the bubbles at the porous sparger, in the same isobutanol solution, is also depicted and it is obvious that no coalescence occurs, although bubbles collide.

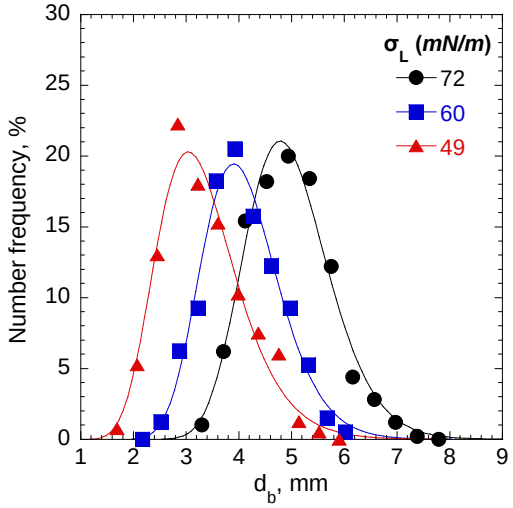

Figure 5: Effect of surface tension on initial size distribution for the porous sparger (Kazakis et al., 2007).

Effect of viscosity

Kazakis et al. (2007) suggested that as viscosity of the liquid phase increases, the Sauter diameter of the bubbles produced by a porous sparger decreases. **Fig. 7** shows the important role that viscosity plays on bubble formation at a porous sparger.

In the present work, the effect of viscosity on bubble formation and the interactions between adjacent growing bubbles has been studied by conducting experiments with various aqueous glycerin solutions. It is known that as viscosity increases, coalescence time also increases (Kim & Lee, 1988), i.e., more time is needed for the liquid film between the bubbles to drain. As already mentioned, coalescence, when glycerin solutions were employed, occurs mainly for the closest tube distance. At larger tube distances, bubbles do not collide at the early stages of their expansion and thus, as they remain in touch for shorter time, before they attain their final size and detach from the tubes, coalescence is less probable.

In order to study the effect of viscosity on bubble coalescence, the coalescence frequency, defined as the ratio of the number of coalescing pairs over the total number of pairs contacted, has been calculated after meticulous observation of the recorded images. **Fig. 8** illustrates the coalescence frequency for all the liquids tested, for various gas flow rates and the distance of 210 μm between the tubes. Four distinct regions can be observed for the glycerin solutions (**Fig. 8**). At very low gas flow rates, i.e., bubble formation frequencies, no coalescence occurs between the contacting bubbles (Region I). As gas flow rate is increased, Region II is observed, at which the coalescence frequency becomes 100%, meaning that every contact between the adjacently growing bubbles leads to coalescence. Region III corresponds to a gas flow rate range at which the coalescence frequency decreases as the flow rate is increased. Finally,

Region IV follows, at which a new slight increase of coalescence percentage is observed with further increase of the gas flow rate.

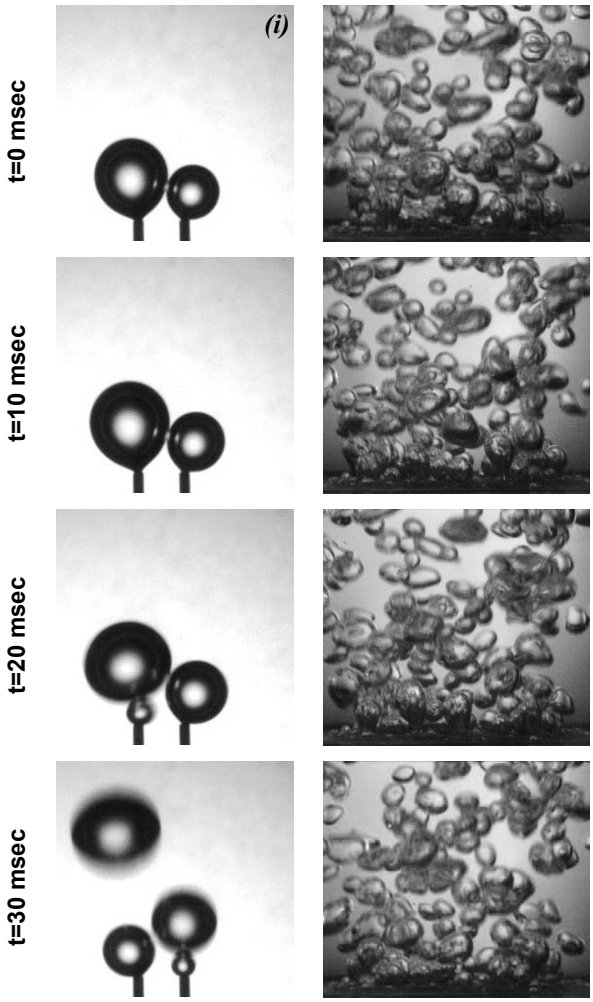

Figure 6: Bubble formation for the: (a) 700 μm tube distance (Q_G=8·10^{-8} m^3/s), *i*, (b) porous sparger, *i* (Kazakis et al., 2007).

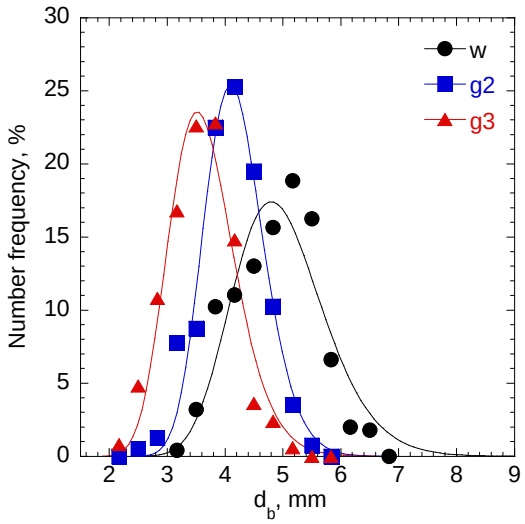

Figure 7: Effect of viscosity on initial size distribution for the porous sparger (Kazakis et al., 2007).

However, water does not follow the general trend of the glycerin solutions, meaning that Regions I and IV are not observed and Region II extends to high gas flow rates. It is also widely known that in water coalescence is instantaneous for two bubbles, i.e., once bubbles collide coalescence occurs even for low gas flow rates.

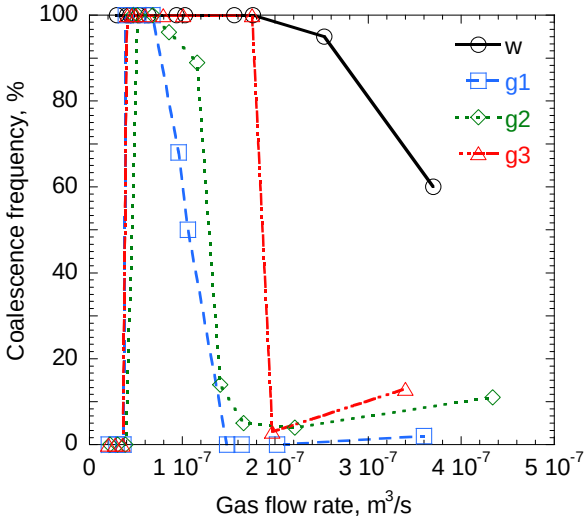

Figure 8: Coalescence frequency versus gas flow rate for all liquids (tube distance: 210 μm).

Fig. 8 also shows the effect of viscosity on bubble coalescence. It is obvious that Region II extends to higher gas flow rates as viscosity increases and that the more viscous the liquid the higher the coalescence frequency, a remark also made by other investigators (e.g. Crabtree & Bridgwater, 1971; Nevers & Wu, 1971; Dekee et al., 1986; Kazakis et al., 2007).

The complexity of bubble coalescence mechanism can be better illustrated in **Fig. 9**, where the formation of two neighbouring bubbles at both the tubes and the porous sparger for two different instances is presented. Although bubbles are formed in the same operating conditions, coalescence does not always take place, indicating that very small fluctuations in the bubble size, the flow rate or the resultant flow field and/or the impact angle of the two bubbles can affect the coalescence probability.

Effect of gas flow rate

As previously stated, the gas flow rate also plays a crucial role in bubble coalescence. The effect of gas flow rate on coalescence between bubbles growing at adjacent tubes can also be seen in **Fig 8**. As already mentioned, there are four different regions of gas flow rate depending on the observed coalescence frequency. At very low gas flow rates no coalescence is observed, although bubbles can be in contact even for 100 msec. However, when Region II is established, coalescence frequency becomes 100 %, eventhough bubbles remain in contact for less than 16 msec. At even higher gas flow rates almost instantaneous coalescence (contact time less than 2 msec) has also been observed. This can be explained by taking into account that: increasing the gas flow rate the expansion velocities of the forming bubbles increase and consequently, the approach velocity also increases. Duineveld (1998) found that when the approach velocity between the colliding bubbles ex-

ceeds a certain value, then bubbles bounce. However, this is not true in the case of under-formation bubbles, which collide while growing at adjacent tubes or pores. As also noted by Tse et al. (1998) the more vigorously bubbles are driven together by the flow, the more rapidly the film drains and the more likely they are to coalesce, especially if they are prevented from bouncing apart, as it happens when bubbles are attached to the tubes or the sparger. The decrease of coalescence frequency after a certain gas flow rate (Region III) can be attributed to the fact that bubbles do not stay in touch for the required time. When gas flow rate is increased, bubbles grow faster and attain their final size in a time less than the coalescence time.

In a similar way, the slight increase of coalescence frequency at very high gas flow rates is ascribed to the high approach velocities between the bubbles leading to the faster draining of the film.

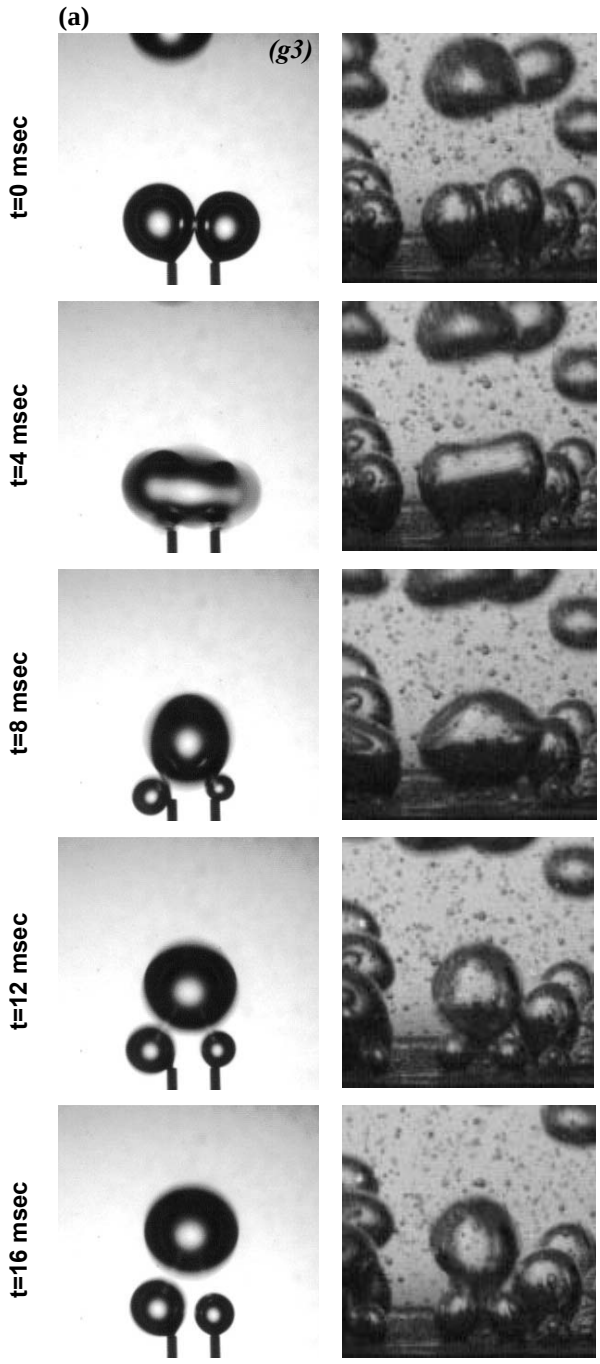

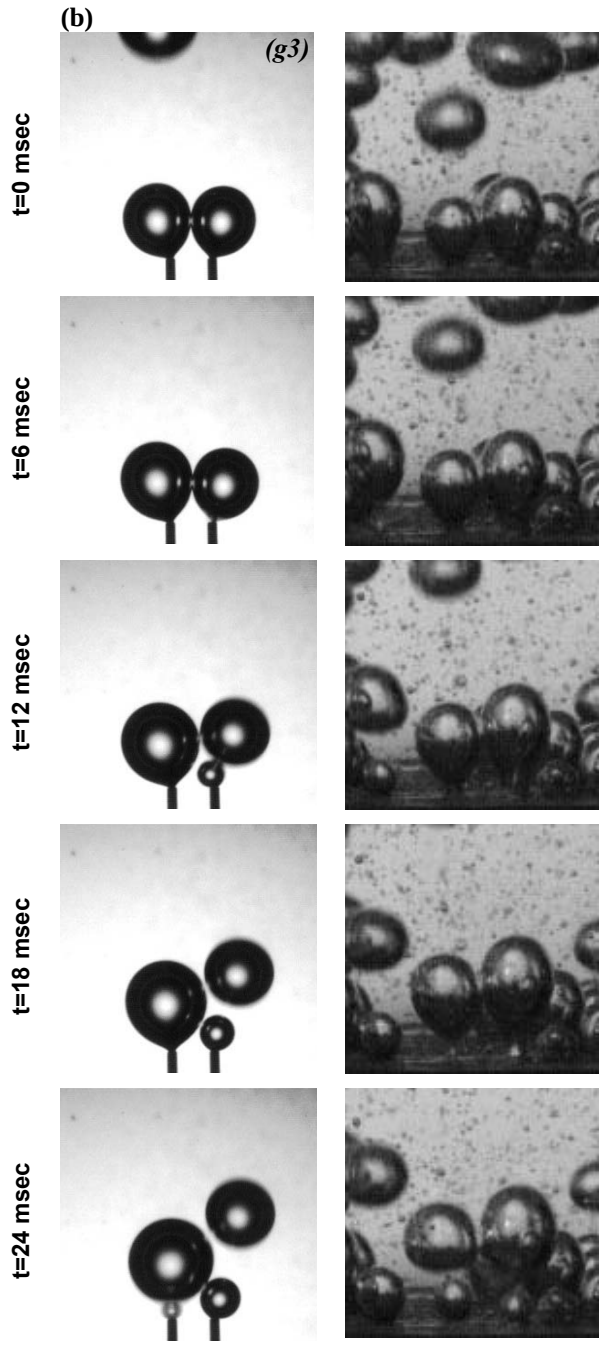

Figure 9: Bubble formation at the tubes and the porous sparger (Kazakis et al., 2007) for *g3*: (a) coalescence occurs, (b) no coalescence occurs; operating conditions between (a) and (b) are the same.

As gas flow rate through the tubes is increased, the gas momentum force (Snabre & Magnifotcham, 1998) acting in the upward direction of the under-formation bubble, also increases leading to higher expansion velocity and, thus, to higher approach velocity between the adjacent bubbles.

Apart from the coalescence type described previously, namely the coalescence between bubbles growing at adjacent sites, another kind of coalescence is also observed during bubble formation near the tube/sparger region.This is the coalescence between the under-formation bubbles and those which have already detached and started to ascend. This interaction occurs at relatively high gas flow rates and it becomes more pronounced after a certain gas flow rate, which depends on the liquid phase employed. It

must be noted that coalescence between forming and ascending bubbles is also observed when a porous sparger is used for the gas dispersion. This kind of coalescence is illustrated in **Fig. 10** for both the tubes and the porous sparger when water is used as the liquid phase.

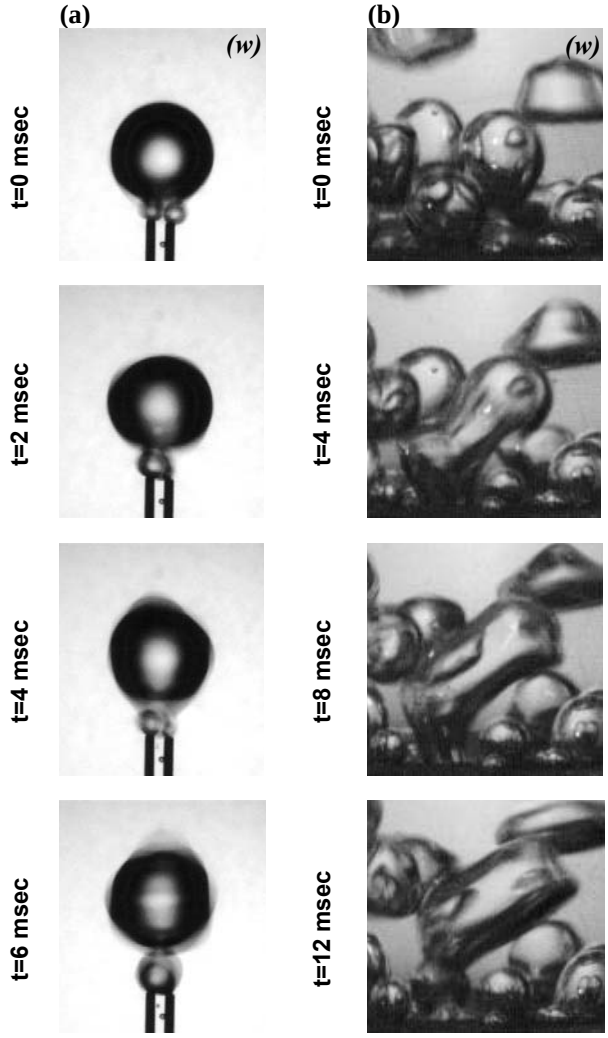

Figure 10: Bubble coalescence between forming and ascending bubble in *w* for the: (a) 210 μm tube distance, (b) porous sparger (Kazakis et al., 2007).

At high gas flow rates, the tubes start to operate more independently, meaning that, since surface tension does not play an important role, bubbles detach earlier being smaller in size and therefore, they cannot collide with neighbouring bubbles. So, it seems that in bubble columns equipped with porous sparger, the appearance of large bubbles at high gas flow rates (heterogeneous regime) is mainly ascribed to this kind of coalescence. At high gas flow rates, coalescence seems to be less pronounced between under formation bubbles, but more intense between the detached bubbles, near the sparger region (at height less than 3 cm) (**Fig. 11**).
It must be also noted that this coalescence takes place at lower gas flow rates as viscosity increases, which is attributed to the lower velocity of the ascending bubbles. As viscosity increases, the detached bubble starts to ascend with a velocity determined by the force balance. However, this velocity is lower due to the increase of the drag force. Consequently, the under-formation bubble catches up with the ascending bubble and after collision, coalescence may occur. **Fig. 12** shows this coalescence in the most viscous liquid studied in the present work.

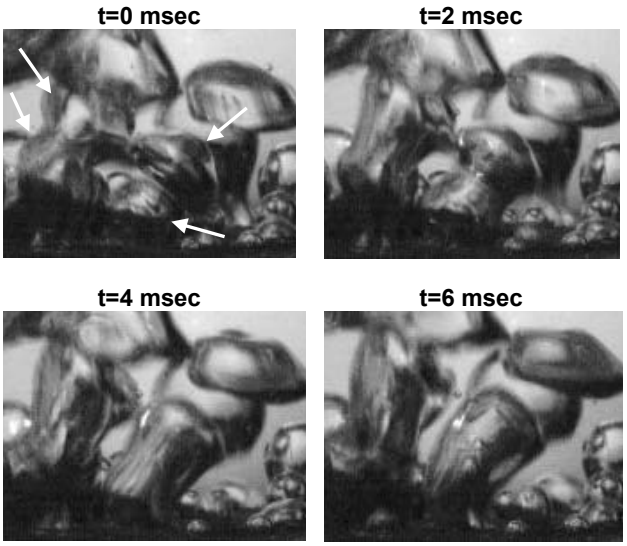

Figure 11: Bubble coalescence between forming and ascending bubble in water at porous sparger at high gas flow rates (Kazakis et al., 2007).

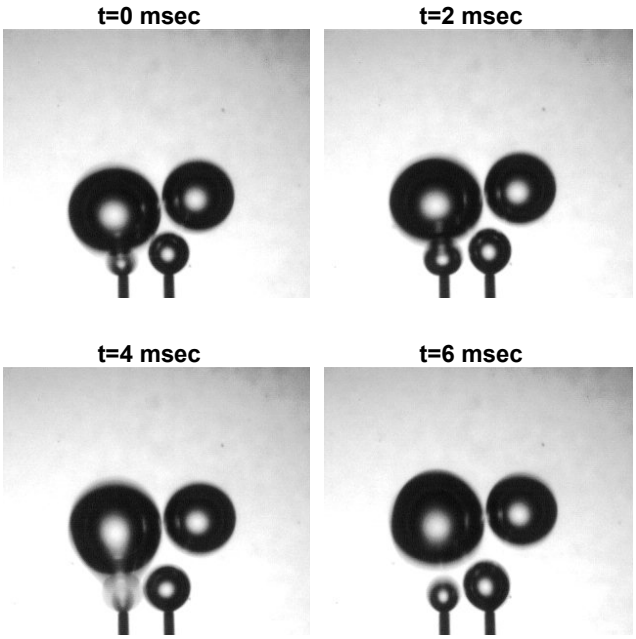

Figure 12: Bubble coalescence between forming and ascending bubble in *g3* and the 700 μm tube distance (Q_G=1.1·10^{-7} m^3/s).

Conclusions

Microscale experiments in a miniature bubble column (cell) were conducted to study the mechanism of bubble creation. Gas was injected through two adjacent tubes, placed at various distances apart from each other, in an effort to simulate the operation of a porous sparger. Various liquids covering a wide range of physical properties have been employed, while a high speed video camera was used in order to obtain an insight into the interactions between

the forming bubbles.
Three different types of coalescence, depending on the distance of the tubes and the instance of bubble expansion at which coalescence takes place, have been observed. The type of coalescence affects the size of the resultant bubbles. When water is used as the liquid phase, a coalescence dependent breakage mechanism was also observed, due to the high level of bubble distortion. The coalescence between two under-formation bubbles may result in the formation of a daughter one, whose size seems to depend on the size of the colliding bubbles.
The coalescence frequency depends on the gas flow rate and four distinct regions can be readily observed. At low gas flow rates no coalescence occurs. At Region II, colliding bubbles always coalesce, while at higher gas flow rate (Region III), the coalescence frequency drops dramatically. At even higher flow rates coalescence frequency slightly increases again. As viscosity increases, the Region II, at which coalescence frequency is 100 %, extends to higher gas flow rates. From the liquids tested, bubbles in the low surface tension isobutanol solution exhibit no tendency to coalesce, regardless of the gas flow rate. On the other hand, when water is used, coalescence always occurs, regardless of the distance between the tubes.
It seems that interactions between bubbles near the region of a porous sparger can be well simulated by the use of two tubes at various distances. However, bubble sizes measured in the present work are about four times smaller compared to those measured by Kazakis et al. (2007) at a porous sparger. This can be attributed to the different way bubbles are connected to the sparger surface, which may extend their resident time and, thus, increase their final size. Consequently, new experiments using a stainless steal plate with very small adjacent holes are needed and are currently in progress in order to simulate more accurate the bubble formation process at a porous sparger.

Acknowledgements

The authors wish to acknowledge the lab technician Mr. A. Lekkas for his contribution to this work.

References

Camarasa, E., Vial, C., Poncin, S., Wild, G., Midoux, N., & Bouillard, J., Influence of coalescence behaviour of the liquid and of gas sparging on hydrodynamics and bubble characteristics in a bubble column. Chemical Engineering and Processing, Vol. 38, 329-344 (1999).

Collela, D., Vinci, D., Bagatin, R., Masi, M. & Bakr, E.A., A study on coalescence and breakage mechanisms in three different bubble columns. Chemical Engineering Science, Vol. 54, 4767-4777 (1999).

Crabtree, J.R. & J., Bridgwater, Bubble coalescence in viscous liquids. Chemical Engineering Science, Vol. 26, 839-851 (1971).

Dekee, D., Carreau, P.J. & Mordarski, J., Bubble velocity and coalescence in viscoelastic liquids. Chemical Engineering Science, Vol. 41, 2273-2283 (1986).

Delhaye, J.-M. & McLaughlin, J.B., Appendix 4: report of study group on microphysics. International Journal of Multiphase Flow, Vol. 29, 1101-1116 (2003).

Duineveld, P.C., Bouncing and coalescence of bubble pairs rising at high Reynolds number in pure water or aqueous surfactant solutions. Applied Scientific Research, Vol. 58, 409-439 (1998).

Kazakis, N.A., Mouza, A.A. & Paras, S.V., Experimental study of bubble formation at porous spargers. Chemical Engineering Journal, submitted.

Kim, J.W. & Lee, W.K., Coalescence behaviour of two bubbles in stagnant liquids. Journal of Chemical Engineering of Japan, Vol. 20 (5), 448-453 (1987).

Kim, J.W. & Lee, W.K., Coalescence Behavior of Two Bubbles Growing Side-by-Side. Journal of Colloid and Interface Science, Vol. 123 (1), 303-305 (1988).

Khurana, A.K. & Kumar, R., Studies in bubble formation – III. Chemical Engineering Science, Vol. 24, 1711-1723 (1969).

Kulkarni, A.A. & Joshi, J.B., Bubble Formation and Bubble Rise Velocity in Gas-Liquid Systems: A Review. Ind. Eng. Chem. Res., Vol. 44, 5873-5931 (2005).

Marrucci, G., A theory of coalescence. Chemical Engineering Science, Vol. 24, 975-985 (1969).

Marrucci, G.. & Nicodemo, L., Coalescence of gas bubbles in aqueous solutions of inorganic electrolytes. Chemical Engineering Science, Vol. 22, 1257-1265 (1967).

Mouza, A.A., Dalakoglou, G.K. & Paras, S.V., Effect of liquid properties on bubble size distribution and gas holdup in a bubble column reactor with fine pore sparger. Chemical Engineering Science, Vol. 60, 1465-1475 (2005).

Noel de Nevers & Jen-Liang, Wu, Bubble coalescence in viscous fluids. AIChE Journal, Vol. 17 (1), 182-186 (1971).

Prince, M.J. & Blanch, H.W., Bubble Coalescence and Break-Up in Air-Sparged Bubble Columns. AIChE Journal, Vol. 36(10), 1485-1499 (1990).

Snabre, P. & Magnifotcham, F.I., Formation and rise of a bubble stream in a viscous liquid. The European Physical Journal B, Vol. 4, 369-377 (1998).

Takahashi, T. & Miyahara, T., Bubble volume formed at submerged nozzles: constant gas flow condition. Kogaku Kogoku Ronbunshu, Vol. 2, 138-143 (1976).

Tsang, Y.H., Koh, Y.H. & Koch, D.L, Bubble size dependence of the critical electrolyte concentration for inhibition of coalescence. Journal of Colloid and Interface Science, Vol. 275, 290-297 (2004).

Tse K., Martin, T., McFarlane, C.M. & Nienow, A.W., Visualisation of bubble coalescence in a coalescence cell, a

stirred tank and a bubble column. Chemical Engineering Science, Vol. 53 (23), 4031-4036 (1998).

Tse K., Martin, T., McFarlane, C.M. & Nienow, A.W., Small bubble formation via a coalescence dependent break-up mechanism. Chemical Engineering Science, Vol. 58, 275-286 (2003).

Valentine, R.S., Sather, N.F. & Heideger, W.J., The motion of drops in viscous media. Chemical Engineering Science, Vol. 20, 719–728 (1965).

Zahradnik, J., Kuncova, G.. & Fialova, M., The effect of surface active additives on bubble coalescence and gas holdup in viscous aerated batches. Chemical Engineering Science, Vol. 54, 2401-2408 (1999).